RSC Advances

RSC Advances

www.rsc.org/advances

ROYAL SOCIETY OF CHEMISTRY

www.rsc.org/advances

Journal Name

ARTICLE

Mechanistic Study of Hydrolytic Degradation and Protonation of Temozolomide

Saber Mirzaei[a], M. H. Khalilian[a], and Avat (Arman) Taherpour[a,b*]

Temozolomide, anticancer and chemotherapy prodrug, undergoes pH dependent ring-opening in both acidic and alkaline conditions. While the rate of degradation accelerates with the increase of the pH, it never comes to a complete halt under acidic mediums. Herein, the temozolomide ring-opening is investigated, in both neutral and acidic conditions, to find out the energy differences and the effects of acidic environment on its activation energy. Two possible different pathways have been considered for ring-opening while compared to path-2, the rate-determining step (first TS) for path-1 is about 15 kcal.mol^{-1} more favourable. However, the second path led to a more stable product. It seems that energy-favoured overall mechanism is a combination of the two paths (tautomerization may occur during process). Moreover, in order to elucidate the role of acidic conditions on more stability and mechanism of the drug, the protonation of all possible sites were examined. This predicts that, protonated oxygen of amide group is the preferable site for protonation that would stabilize the system by about 1.23 kcal.mol^{-1} more than the next favourable protonation site (protonated nitrogen in imidazole ring). The low energy barrier (6 kcal.mol^{-1}) for proton exchange in these two sites results in simultaneous existence of both N-protonated and O-protonated structures. Additionally, the pK$_a$ values were calculated and averaged out at -2.625. This value implies the extreme acidic feature of protonated temozolomide that does not protonate or deprotonate in normal pH range. The protonation and mechanism of degradation process were treated using density functional theory (B3LYP) and by employing complete basis set (CBS-4M) method. Also, high-level G3MP2 level was used on occasion.

Introduction

As an antitumor prodrug, Temozolomide (TMZ) has attracted a lot of attention due to its decomposition mechanism and advantages over the previous alkylating agents (e.g. dacarbazine and mitozolomide). As a prototype of TMZ, Mitozolomide (MTZ) exhibits toxic side effects and fails to pass the phase II of clinical trials.[1] Now TMZ is the only alkylating agent of imidazotetrazine series that is being used for treatment of a wide spectrum of malignant, gliomas and some kinds of skin cancers.[2-5]

The activation mechanism of TMZ has been rationalized by means of NMR spectroscopy.[6-7] TMZ tetrazinone ring-opening, which eventuates in the complete degradation of system, begins with the addition of a water molecule to carbonyl moiety. Subsequently, by CO_2 elimination, the intermediate bioactive molecule (MTIC) will be generated. Thereafter, MTIC undergoes decomposition and releases methylating species (methyldiazonium ion) and by-product AIC. The mechanism of degradation is highly pH sensitive. The rate of TMZ degradation increases with the increase of the pH.[6] TMZ half-life in phosphate buffer with physiological pH (7.4) is around

1.83 hour[6] whereas, the stability of drug in acidified human plasma (pH<4) increases to about 24 hour.[8]

The chemical stability of the TMZ has been the issue in prolonged storage. The colors of the pure TMZ crystals fade from white to pink and then light brown in spontaneous degradation. Complete color change in the white crystals of TMZ has been seen after 4 hours for drugs stored at 45% relative humidity.[9] In order to prevent the spontaneous degradation and enhance the stability of the drug several co-crystals of TMZ have been studied.[10-13] Also, nine TMZ polymorphs and a system, which extends the drug stability for prolonged storage were reported in patent literature.[9,14] TMZ cocrystal with Anthranilic acid with pK$_a$ 4.95 is stable for two weeks, which is one week more in comparison to TMZ at the same conditions.[10] The stability of TMZ-Saccharin co-crystal (pK$_a$ 2.3) is around two months at the ambient conditions.[11] Also, the acidified temozolomide-H+Cl- were reported. The first crystallization of protonated TMZ was published in 1995 and the structure of protonated species was ascertained based on the ^{15}N chemical shifts.[15] Later in 2013 Babu et al. reported the crystallographic data of protonated form of TMZ and rationalized their evidence based on the calculated pK$_a$s using
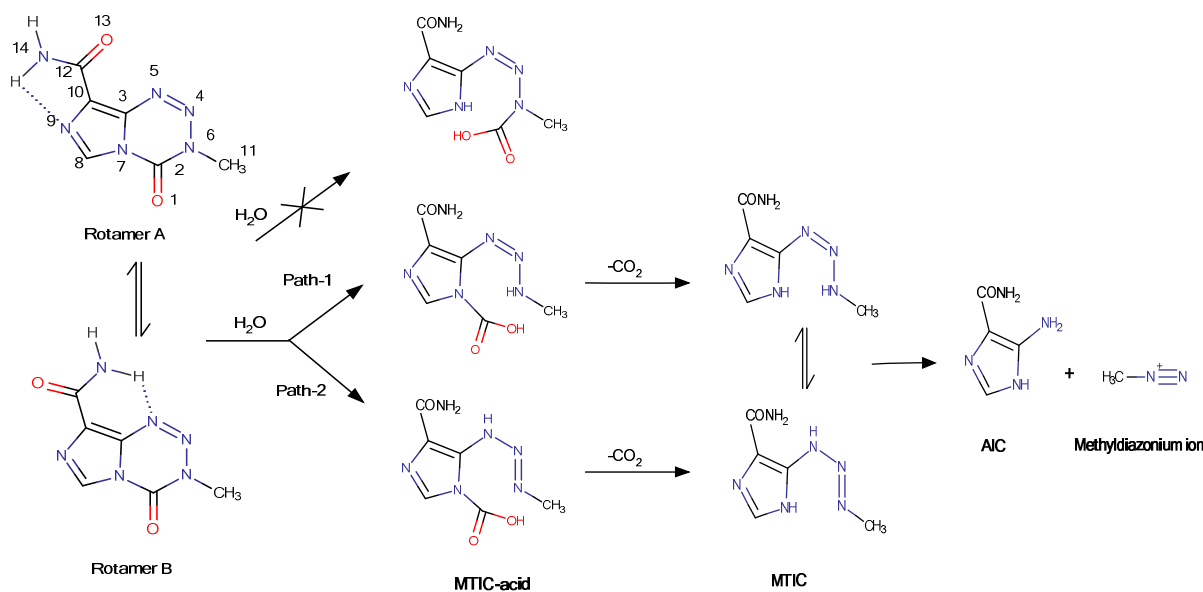
Scheme 1 The different pathways for Temozolomide direct hydrolysis.

ChemAxon's Marvin software.[16] They mentioned the poor and twinned quality of obtained crystals and also the bounded hydrogen atom to N and O, which was located in different Fourier maps.[17] Thus, because of the ambiguities mentioned for best protonation site and to seek the protonation effect on TMZ decomposition, the protonated structures with their energies accompanied by pK_a values were obtained using quantum chemical approach.

In addition, Kasende and coworkers have investigated the interaction of water molecule with TMZ theoretically and predicts that carbonyl O is preferred over other N atoms to binds to water molecule.[18] However, the acidified structures were not addressed in this work and they only content to study the TMZ binding site with NBO data. Also, it is worthy to note that, TMZ is highly unstable in water media, so only considering the favoured binding site with water molecule without examining its degradation would be misleading.

This article is aimed to study the TMZ degradation mechanism in both neutral and acidic conditions to find its decomposition paths, provide insights into its pH dependence behavior and the stability of the drug, which could be applicable for preparation of novel pharmaceutical co-crystals of TMZ.

Methodology

Complete optimization of all structures has been done by density functional theory and complete basis set (CBS-4M)[19] methods. DFT calculations were carried out using B3LYP[20] functional with 6-31+G(d) and 6-311++G(2d,p) basis sets for

mechanism and protonation studies, respectively. The mentioned methods show good result in some structural-like cases.[21] Furthermore, several studies examine the protonation effect at $G_n(MP2)$ levels, so for the sake of accuracy the G3MP2[22] method was also selected for obtaining protonation energies.[23-25] It is good to note that higher level CBS-QB3 method was not used instead of CBS-4M owing to its limitation to compounds with less or near 10 heavy atoms (TMZ+water has 15 heavy atoms).[26]

In order to confirm the exact structure of reactants, transition states, and products, the vibrational frequencies were examined. One imaginary value was observed for all transition states; subsequently, intrinsic reactant coordinate (IRC) calculations were used to assure the presence of correct optimized transition states. The reactant and product of IRC calculation were optimized further by the same method. Also, integral equation formalism variants of the polarizable continuum model (IEF-PCM)[27] with UFF radii were used to study the solvent effects on the optimized structures. Other solvation model SM8 was considered to see the difference between these solvation approaches[28]. This universal solvation model (SM8) also has been used for pK_a calculation. This model is known for giving very precise pK_a values[29] (complete procedure for obtaining pK_a data was summarized in supplementary information).

For TMZ decomposition mechanism studies, the complex of TMZ+water (optimized as one system) was selected as reference compound (G_{ref}), and other energies were calculated relative to it, using the $\Delta G = G_{ref} - G_x$ equation (see table 1).

The absolute free energies (G) are also provided in the supplementary information.
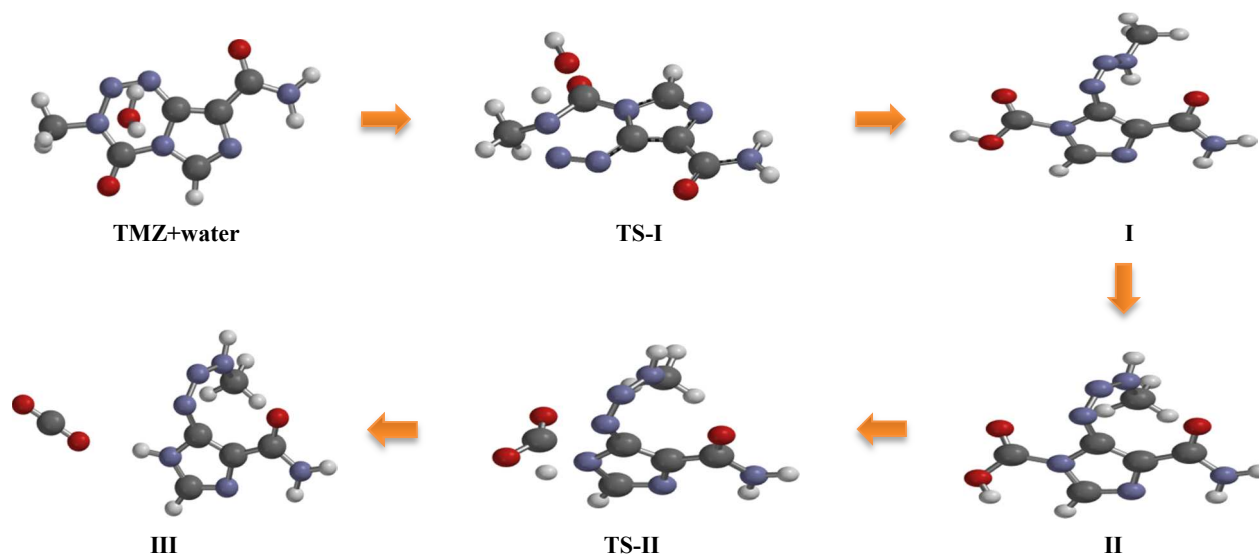
Figure 1 Path-1: TMZ decomposition
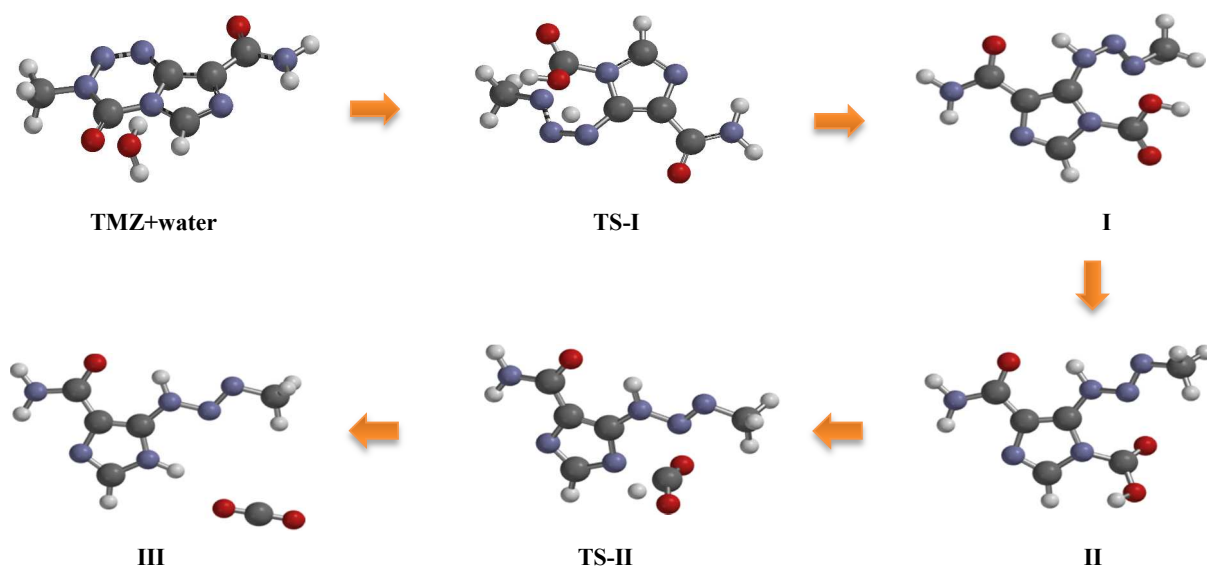
Figure 2 Path-2: TMZ decomposition

Reactivity and electrophilicity of TMZ species were considered using the following standard equations:

$$\eta = E_{LUMO} - E_{HOMO}$$

$$X = -(E_{LUMO} + E_{HOMO})/2$$

$$\omega = X^2 / 2\eta$$

$$N = 1/\omega$$

Ŋ, X, ω and N denotes hardness, electronegativity, global electrophilicity and nucleophilicity index, respectively. The charge distribution data was achieved using natural population analysis (NPA) approach[30] by the B3LYP/6-311++G(2d,p) method. Likewise, the nuclear independent chemical shifts

(NICSs)[31] were calculated by employing GIAO[32] method and using B3LYP/6-311++G(2d,p) level. All the investigations were executed with Gaussian 03 and Spartan 10 software packages.[33-34]

Results and discussion

Hydrolytic degradation mechanism of TMZ to MTIC

The 2D pathways of this reaction have been summarized in scheme 1. TMZ can react with a water molecule to initiate its degradation and generate MTIC-acid. This step passes from first transition state (TS-I in figure 1). There are two ways for opening TMZ tetrazinone ring (N6-C2 and N7-C2). Although, both N6-C2 and N7-C2 bonds weakens (longer bonds) during ring-opening[35], but all attempts to find transition state for N7-C2 ring-opening using both CBS-4M and DFT levels were aborted. This may due to the electron donating effect of methyl group, which cause the ring-opening to occur via cleavage of N6-C2 bond. This N6-C2 bond cleavage can proceed through two different pathways (path-1 and path-2) to form MTIC-acid, which then releases CO_2 molecule and generates MTIC. The produced MTICs from path-1 and path-2 are tautomer forms, while the water-mediated energy barrier for this 1,3 hydrogen shift is 5.93 kcal.mol^{-1}.[36] The energy diagram for both paths revealed that in spite of lower TS-I for path-1, the TS-II and obtained products are more energy favoured for the second path. It appeared that the TMZ would prevail over ring opening in more energy favoured path-1 that forms the first MTIC tautomer but then undergoes tautomerism to generate MTIC next tautomer (scheme 1), which decomposes through the second path. The overall mechanism for this sequence was depicted in supplementary information.

Since TMZ has two rotamers, their difference is 1.35 kcal.mol^{-1} at G3MP2 (based on the calculated free energy), the two proposed paths were investigated for the both rotamers. This marginal more stability of rotamer A can be explained by aromaticity index and may attribute to the more negative charge of N9 (-0.476) compared with the N5 (-0.237). Here the nucleus-independent chemical shifts (NICSs) were calculated for both five-membered and six-membered rings; also the NICSs for pseudo-ring of both rotamers that are the result of intra-hydrogen bond have been estimated. Although, NICSs are almost same for the rings, but this value for rotamer A (C10-C12-N14-H…N9) and rotamer B (C3-C10-C12-N14-H…N5) pseudo-rings are -0.484 and +1.674 respectively. The negative values of NICS indicate the aromaticity and positive values denote the anti-aromaticity feature of that ring. This more aromaticity along with the more negative charge of N9 could justify the more stability of rotamer A.

Note that the transition energy difference for both rotamers is roughly the same, so on the basis of Curtin-Hammett principle, the product can be derived from either rotamers and the conformational equilibrium does not alter the product distribution. Owing to this reason, only the first rotamer of TMZ has been reported in the main text and energy diagrams for the second rotamer are given in supplementary information.

Path-1 mechanism

The path-1 consists of a two-steps mechanism, the first step (TS-I) is the rate determining step, which is in agreement with experimental results obtained by Denny et al. reminding that the rate-determining step must be at the early stage of the TMZ overall decomposition[6]. In this two-steps pathway, one proton is transferred from the water molecule to N6 of tetrazinone ring to produce the first transition state (the forming N-H distance is 1.18 Å and the breaking bond length (O-H) is 1.37Å). Subsequently, oxygen of H_2O simultaneously attacks the carbonyl carbon (C2) to open the ring from C2-N6 bond. The C2-O bond forming length is 1.89Å and C2-N6 distance is 1.55Å, which is longer than C2-N6 bond (1.27Å) in TMZ. Base on the IRC calculations, TS-I connect the complex of TMZ and H_2O to MTIC-acid (figure 1). The gas phase relative Gibbs free energy barrier for TS-I of Path-1 is 57.56 kcal.mol^{-1} at B3LYP and 62.89 kcal.mol^{-1} at CBS-4M (figure 3 and table 1). The transition energies in water media for both PCM and SM8 solvation models have been also reported in table 1, which shows little change with respect to gas data. First transition state for rotamer B is marginally different (supplementary information). In the second transition state (TS-II) one proton is transferred from OH to N7 to form complex of MTIC and carbon dioxide. In TS-II, the N7-H forming bond length is 1.32 Å. The N7-H bond formation in TS-II is simultaneous with C2-N7 bond breaking The C2-N7 bond length is 1.77 A. The energy barrier for this transition is about 38.59 kcal.mol^{-1}, which compared to first TS is ~20 kcal.mol^{-1} lower. The energy profile for this two-step degradation is illustrated in figure 3.
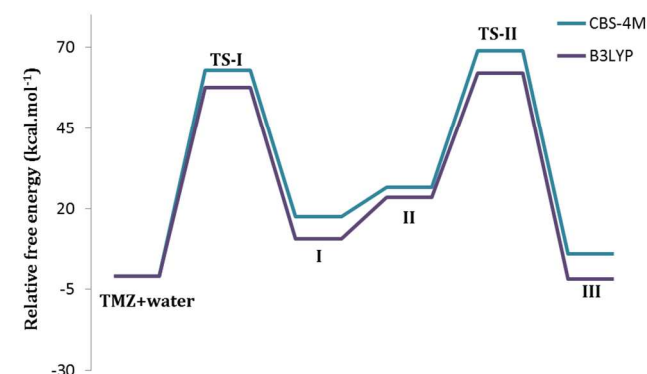
Figure 3 The path-1 relative energy profile of TMZ decomposition in vacuo.

Path-2 mechanism

With regard to path-1, the second path of tetrazinone ring opening also includes two steps. A proton transfer from H_2O to N5 of tetrazinone ring initiates the ring opening. Subsequently, the transfer of proton to N5 leads to formation of N4-N6 double bond. Thereafter, the C2-N6 bond is collapsed as the MTIC-acid is formed. This stage of the mechanism produces the first transition state (TS-I). In TS-I the N5-H bond length is 1.26 A, and the O-H distance is 1.34 A. The N5-N4, N4-N6 and N6-C2

Table 1 The calculated relative free energies (ΔG) for both TMZ degradation paths (in kcal.mol^{-1})

Structure[a]	PATH-1				PATH-2			
	CBS-4M (gas)	B3LYP/6-31+g* (gas)	B3LYP/6-31+g* (PCM)	B3LYP/6-31+g* (SM8)	CBS-4M (gas)	B3LYP/6-31+g* (gas)	B3LYP/6-31+g* (PCM)	B3LYP/6-31+g* (SM8)
SR[b]	-2.75	-4.15	-8.26	-7.89	-2.75	-4.15	-8.26	-7.89
TS-I	62.89	57.56	57.59	59.35	77.04	72.10	69.27	70.17
I	17.41	10.61	10.52	13.71	7.11	3.75	7.33	8.75
II	26.59	23.58	20.60	20.99	13.45	8.42	10.09	9.43
TS-II	68.97	62.17	63.31	64.30	52.26	43.16	48.79	48.14
III	5.89	-1.74	-2.89	3.94	-8.82	-20.93	-17.74	-10.18

[a] The TMZ+water structure has been optimized as a reactant and all other energies were compared to this structure relatively. [b]Separated reactants.

bond lengths in transition state are 1.38 A, 1.27 A and 1.60 A, respectively, whereas, these values in intact TMZ are 1.27, 1.37 and 1.38 Angstrom, respectively. Decreasing the value of N4-N6 from 1.37 to 1.27 A indicates the formation of double bond. The barrier height of first transition state is estimated to be 72.10 kcal.mol^{-1} at B3LYP level, which is approximately 15 kcal.mol^{-1} more than the TS-I in path-1 (figure 3 and 4). In table 1 the TMZ+water (treated as a system) has been chosen as the base compound and the energy of other compounds were compared with this system (absolute free energies were given in supplementary information). Inclusion of water solvent keeps this energy deference at about 13 kcal.mol^{-1}. The TS-1 energy barrier for the TMZ second conformer is almost the same (supplementary information). For the second step of the mechanism, the acid proton transfers to N7 of imidazole ring to form second transition state (TS-II). The N7-C2 bond length is 1.89 A, which is somewhat longer than the N7-C2 bond length of path-1 (1.77 A) second transition state. The O-H breaking bond is 1.19 A. The first transition state for path-2, like path-1, is the rate determining step. The TS-II of path-2 has lower energy barrier (~5 kcal.mol^{-1} and also ~5 kcal.mol^{-1} in gas and aquase phase) in comparison to the TS-II of path-1. This indicates that path-2 is preferred over path-1 with respect to second step of the mechanism. Also, from thermodynamic view the path-2 lead to a more stable product (table 1).
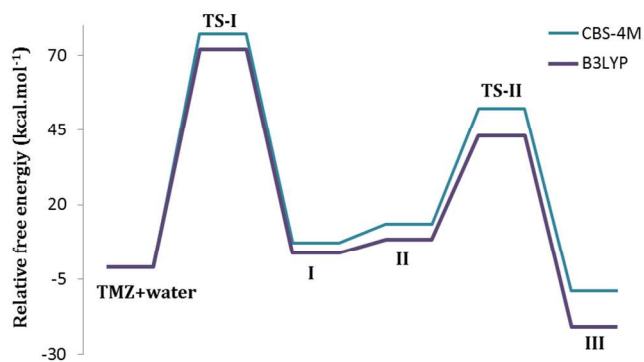
Figure 4 The path-2 relative energy profile of TMZ decomposition in vacuo

Protonation of temozolomide

To probe a relation between the energy barriers of TMZ decomposition and pH, first, protonation energies were investigated for both rotamers of TMZ A and B using multiple methods listed in table 2. In spite of the previous reported studies, which predicted the nitrogen atom in imidazole ring (N9) for best protonation site, the obtained values for protonation energies demonstrated that protonation of oxygen atom in TMZ amide group (O13) would be a more favourable

Table 2 Protonation free energies (ΔG) of TMZ (in kcal.mol^{-1})

Protonated atom*	B3LYP/ 6-311++G(2d,p)		CBS-4M		G3MP2	
	TMZA	TMZB	TMZA	TMZB	TMZA	TMZB
O13	-217.8	-219.4	-215.9	-217.7	-217.4	-218.7
N9	-205.7	-217.2	-205.1	-216.6	-204.8	-216.4
N5	-210.6	-196.1	-209.3	-195.2	-208.8	-194.2
O1	-186.4	-184.0	-183.5	-180.6	-186.4	184.0

*The free energies of the other atoms were given in supplementary information.

process by 2.23 kcal.mol^{-1} at G3MP2 for TMZ B (N9 protonated TMZ B is more stable than A due to the less steric hindrance and intra-hydrogen bond). Moreover, the obtained charge distribution, which has been achieved through the use of NPA, showed that more negative charge is present on O13 (-0.596). The pK$_a$ is -2.47, -2.78 for O13 and N9, respectively (the Pk$_a$ values were calculated using the procedure and method described in supplementary information). These very close values can be settled by the fact that these two protonation sites can interchange the proton between each other. The O13 and N9 protonated species may convert to each other by a relatively low barrier height (13.14 kcal.mol^{-1}) that could rationalize the simultaneous presence of both species (figure 5). Therefore, the pK$_a$ values also have been averaged out for both N9 and O13 at about -2.625. The negative value for pK$_a$ clearly indicates that

O13= **0.00** (0.00) [0.00]   TS-1= **13.14** (12.61) [12.27]   N9= **2.33** (1.11) [2.23]

O13w = **0.00** (0.00) [0.00]   TSw= **6.06** (5.11) [4.14]   N9w= **1.23** (-0.87) [0.88]
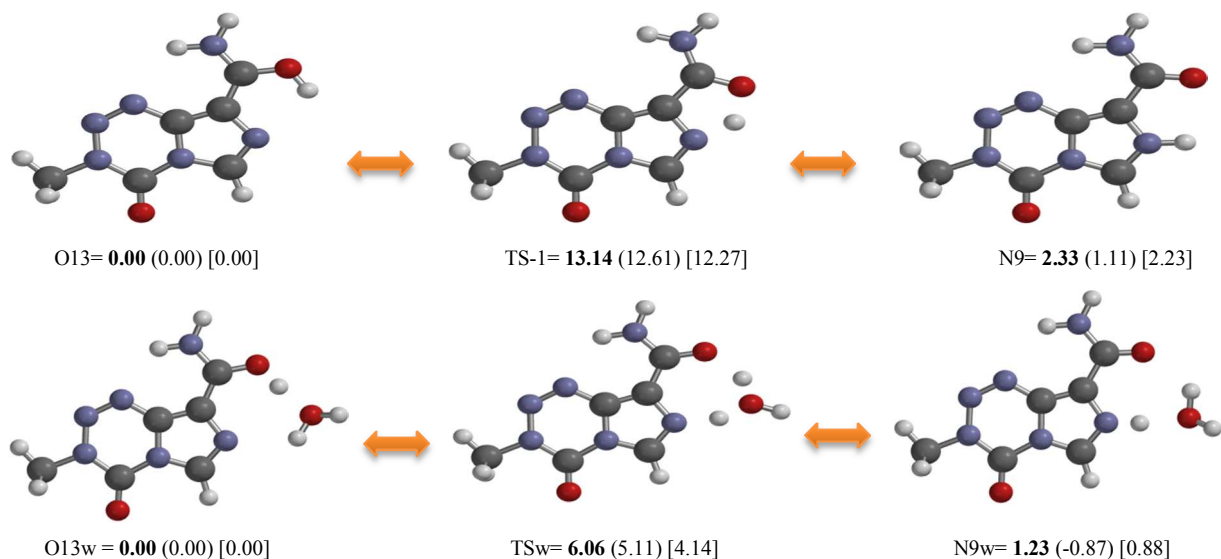
Figure 5 The gas and water-mediated interconversion between N9 and O13 protonated forms of Temozolomide. Values in bold, in parentheses, and in square bracket are the calculated relative ΔG (kcal.mol⁻¹) at G3MP2, CBS-4M, and B3LYP/6-311++G(2d,p) methods respectively.

Table 3 Highest Occupied Molecular Orbital (HOMO) energy- Lowest Unoccupied Molecular Orbital (LUMO) energy - Hardness Ƞ- Electronegativity X- Global electrophilicity ω, and Nucelophilicity Index N. all data calculated at b3lyp/6-311++G(2d,p)

Molecule	HOMO (au)	LUMO (au)	Ƞ (eV)	X (eV)	ω (eV)	N (eV)	TS*
TMZ-A	-0.2651	-0.1016	4.449	2.225	15.130	0.066	59.2
TMZ-B	-0.2682	-0.1103	4.296	2.148	14.613	0.068	60.4
O13-A	-0.4177	-0.2672	4.096	2.047	13.905	0.072	62.0
O13-B	-0.4170	-0.2670	4.081	2.040	13.878	0.072	63.3
N9-B	-0.4367	-0.2658	4.649	2.325	15.820	0.063	61.4

*Gibbs free energies of rate determining (TS-I of path-1), at b3lyp/6-311++G(2d,p)

TMZ only would protonated in extremely acidic conditions. In addition, as illustrated in figure 5, incorporation of explicit water molecule would decrease this barrier to 6.06 kcal.mol⁻¹. So, the two protonated species would interconvert rapidly in aqueous phase. Water molecule also decreases the energy difference between O13w and N9w protonated structures (absolute free energies were given in supplementary information).

Reactivity of TMZ in both acidic and basic condition

The reactivity of TMZ can be assessed by using its relationship with electrophilicity-nucleophilicity. This concept calculates the global (ω) or local electrophilicity and nucelophilicity Index (N) with employing several standard equations, which are given in methodology section. This method for calculating reactivity has been used by several various groups.[37-41]
The obtained results from these equations for conformer A and B of neutral and O13 protonated TMZ with the N9 protonated

species were reported in table 3. The values of global electrophilicity reveal the extreme attitude of both neutral and protonated TMZ (strong acidic condition) toward nucleophiles. The protonation has trivial effects on the electrophilicity of TMZ (protonation on O13 lowers the electrophilicity to some extent). Also, the partial atomic charges supported the results of table 3. The calculated charges (supplementary information) indicate that the C2 has the biggest positive charge (+0.830) in TMZ, which could be attributed to the attachment of three electron-withdrawing atoms to it. Moreover, the first transition state (TS-I of path-1) of TMZ hydrolytic degradation on the more favourable protonated species was repeated. The N9 protonation increases the barrier of TS-I around 1 kcal.mol⁻¹. These values for protonation at O13 are 2.8 kcal.mol⁻¹ and 2.9 kcal.mol⁻¹ for O13-A and O13-B, respectively. This also can be seen qualitatively from figure 6, which demonstrates the LUMO orbitals of TMZ and its O13 protonated (these LUMO orbitals considered to be attacked by nucleophiles). The contribution of C2 in LUMO orbital of O13 protonated structure is less than its unprotonated TMZ (figure 6), so as expected, the nucleophile attack at C2 is more convenient in TMZ unprotonated structure. From all these data, it concluded that protonation (lower pH) decrease the rate
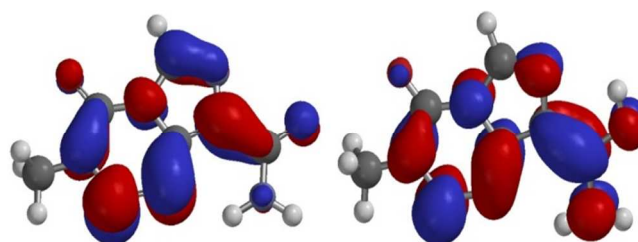
Figure 6 LUMO orbital of TMZ (left) and O13 protonated TMZ (right).

of the reaction marginally, but does not completely halt its decomposition. Also, the extreme high protonation energy of O1, around 31 kcal.mol^{-1} more than the O13 (see table 2), is the other factor contributing to the rate decline, which takes away the possibility for acid catalyst degradation.

Finally, a brief description of basic media effects on decomposition energies was considered using hydroxide ion in order to give a better perspective of the TMZ degradation. The alkaline conditions diminish the energy barrier for degradation dramatically to about 20.58 and 7.23 kcal.mol^{-1} in TS-I (Two different transition states were found). This justifies the degradation rate of TMZ increases from acid to basic condition. Also, in order to considering the effects of other nucleophiles on the TMZ decomposition, the first transition state of path-1 was determined for nucleophiles methylamine (MeNH$_2$), methanol (MeOH), and acetic acid (CH$_3$COOH). The barrier of the rate determining step (TS-I of path-1) is approximately same for these three molecules (53-56 kcal.mol^{-1}). However, it seems that their transition state barrier is lower than water media, it has been reported that the rate of TMZ degradation to AIC reduce in media like methanol (the rate of methanolysis is ~2-3 days in comparison to less than one day for hydrolysis).[10] About the acetic acid, the optimized structure of product prefer to retain its cyclic form and shows insignificant signs of ring opening. The product is around the 40.11 kcal.mol^{-1} less stable than reactants (this value in water media has obtained 17.41 kcal.mol^{-1} (figure 3)), this large instability decrease the reverse transition state barrier to around 15 kcal.mol^{-1}, which could overcome the forward path dramatically (55 kcal.mol^{-1}). This could be another reason for the more stability of TMZ in acidic condition. Nevertheless, the role of the more acetic acid lipophilicity rather than water should not be ignored. The complete data for these computations were given in the supplementary information.

Conclusions

The degradation reaction of anticancer TMZ drug was simulated by the use of quantum chemical methods. The former mechanistic studies of TMZ focused more on the base-catalyst path; hence the neutral and acidic conditions were explored here (for comparison basic media was also considered briefly).The obtained results demonstrate that this decomposition is a two-pathway reaction in which the rate determining step (TS-I) for path-1 is lower than the second path. Nevertheless, it does not mean that TMZ would be merely decomposed through path-1 as the path-2 has more stable TS-II and products. Thus, it has been suggested that TMZ would prevail over TS-I in much more favourable path-1 but then tautomerized to continue its degradation through the second path (the two paths differ in generated MTIC-acid tautomeric form). Additionally, to take the acidic effects on overall reaction into account, the protonation energies for all atoms were calculated. A novel most stable protonated form, O13 protonated, was identified, which interconverts rapidly with the next preferred protonation site (reported by previous studies). Repeated calculations on achieved protonated structures of rate determining step of TMZ

mechanism revealed that the protonation has a decreasing effect on TMZ reactivity. However, the mechanism in neutral and near acidic mediums signifies that the decomposition would occur, but at a lower rate than more common base-catalyzed. The parallel acid-catalyzed did not participate in decomposition procedure, that it would equal the rate in both acidic and basic conditions, owing to the large protonation energy for O1. In addition the electrophilicity and nucleophilicity index were investigated to support these consequences.

Acknowledgements

Notes and references

a. Faculty of Chemistry, Razi University, P. O. Box: 67149-67346, Kermanshah, Iran.
b. Medical Biology Research Center, Kermanshah University of Medical Sciences, Kermanshah, Iran. E-mail: avatarman.taherpour@gmail.com; Tel.-Fax.: +98(83)34274559.

1. E. S. Newlands, G. Blackledge, J. A. Slack, C. Goddard, C. J. Brindley, L. Holden, M. F. Stevens, Cancer Treat Rep. 1985, **69**, 801.
2. H. S. Friedman, T. Kerby, H. Calvert, Glioma. Clin. Cancer Res. 2000, **6**, 2585.
3. M. J. van den Bent, M. J. Taphoorn, A. A. Brandes, A. A. J. Clin. Oncol. 2003, **21**, 2525.
4. I. Quirbt, S. Verma, T. Petrella, K. Bak, M. Charette. Curr. Oncol. 2007, **14**, 27.
5. W. J. Hwu. Oncol. (Williston Park). 2000, **14**, 25.
6. B. J. Denny, R. T. Wheelhouse, M. F. G. Stevens, L. L. H. Tsang J. A. Slack. Biochemistry. 1994, **33**, 9045.
7. R. T. Wheelhouse and M. F. G. Stevens. J. Chem. Soc., Chem. Commun., 1993, 1177.
8. H. Kim, P. Likhari, D. Parker, P. Statkevich, A. Marco, C. Lin, A. A. Nomeir. Journal of Pharmaceutical and Biomedical Analysis. 2001, **24**, 461.
9. O. Braverman, R. Feishtein, A. Weisman, J. Kaspi. US Pat., 0222792 A1, Oct. 05, 2006.
10. N. J. Babu, P. Sanphui, A. Nangia. Chem. Asian J. 2012, **7**, 2274.
11. N. J. Babu, L. S. Reddy, S. Aitipamula, A. Nangia. Chem. Asian J. 2008, **3**, 1122.
12. P. Sanphui, N. J. Babu, A. Nangia. Cryst. Growth Des. 2013, **13**, 2208.
13. A. Nangia, N. J. Babu, P. Sanphui, WO Pat., 036676 A2, Mar. 31, 2011
14. I. Adin, C. Iustain, US Pat., 0187206 A1, Aug. 25, 2005.
15. R. T. Wheelhouse, D. E. V. Wilman, W. Thomson, M. F. G. Stevensa. Chem. Soc. Perkin Trans. I, 1995, 249.

ARTICLE

16. pK$_a$ calculator, Marvin 5.10.1, 2012, ChemAxon, http://www.chemaxon.com.
17. N. J. Babu, P. Sanphui, N. K. Nath. U. V. R. Khandavilli, A. Nangia. CrystEngComm. 2013, **15**, 666.
18. O. E. Kasende, A. Matondo, M. Muzomwe, J. T. Muya, S. Scheiner. Comp. Theor. Chem. 2014, **1034**, 26.
19. G. A. Petersson, J. A. Montgomery, M. J. Frisch, J. W. Ochterski. J. Chem. Phys. 2000, **112**, 6532.
20. A. D. Becke. J. Chem. Phys. 1993, **98**, 5648.
21. D. L. Cao, F. D. Ren, J. L. Wang, W. L. Wang. J. Mol Struc. THEOCHEM. , 2007, **805**, 53.
22. L. A. Curtiss, P. C. Redfern, K. Raghavachari, V. Rassolov, J. A. Pople. J. Chem. Phys. 1999, **110**, 4703.
23. P. J. Amorim Madeira, P. D. Vaz, R. J. N. Bettencourt da Silva, M. H. Florêncio. ChemPlusChem, 2013, **78**, 1149.
24. S. Gronert, D. C. Simpson, K. M. Conner, J. Am. Soc. Mass. Spectrom. 2009, **20**, 2116.
25. P. V. Bharatam, D. S. Patel, P. Iqbal. J. Med. Chem. 2005, **48**, 7615.
26. G. A. Petersson, J. A. Montgomery Jr, M. J. Frisch, J. W. Ochterski, J. Chem. Phys. 2000, **112**, 6532.
27. M. T. Cance`s, B. Mennucci, J. Tomasi. J. Chem. Phys. 1997, **107**, 3032.
28. A.V. Marenich, R. M. Olson, C. P. Kelly, C. J. Cramer, D. G. Truhlar, J. Chem. Theory Comput. 2007, **3**, 2011.
29. S. Gangarapu, A. T. M. Marcelis, H. Zuilhof, ChemPhysChem, 2013, **14**, 990.
30. A. E. Reed, R. B. Weinstock, F. J. Weinhold. Chem. Phys. 1985, **83**, 735.
31. P. V. R.; Schleyer, C. Maerker, A. Dransfeld, H. Jiao, J. Am. Chem. Soc. 1996, **118**, 6317–6318.
32. F. London, J. Phys. Radium. 1937, **8**, 397.
33. Frisch, M. J.; Trucks, G. W.; Schlegel, H. B.; Scuseria, G. E.; Robb, M. A.; Cheeseman, J. R.; Montgomery, J. A.; Vreven, T., Jr.; Kudin, K. N.; Burant, J. C.; Millam, J. M.; Iyengar, S. S.; Tomasi, J.; Barone, V.; Mennucci, B.; Cossi, M.; Scalmani, G.; Rega, N.; Petersson, G. A.; Nakatsuji, H.; Hada, M.; Ehara, M.; Toyota, K.; Fukuda, R.; Hasegawa, J.; Ishida, M.; Nakajima, T.; Honda, Y.; Kitao, O.; Nakai, H.; Klene, M.; Li, X.; Knox, J. E.; Hratchian, H. P.; Cross, J. B.; Adamo, C.; Jaramillo, J.; Gomperts, R.; Stratmann, R. E.; Yazyev, O.; Austin, A. J.; Cammi, R.; Pomelli, C.; Ochterski, J. W.; Ayala, P. Y.; Morokuma, K.; Voth, G. A.; Salvador, P.; Dannenberg, J. J.; Zakrzewski, V. G.; Dapprich, S.; Daniels,A. D.; Strain, M. C.; Farkas, O.; Malick, D. K.; Rabuck, A. D.;Raghavachari, K.; Foresman, J. B.; Ortiz, J. V.; Cui, Q.; Baboul, A. G.; Clifford, S.; Cioslowski, J.; Stefanov, B. B.; Liu, G.; Liashenko, A.; Piskorz, P.; Komaromi, I.; Martin, R. L.; Fox, D. J.; Keith, T.; Al-Laham, M. A.; Peng, C. Y.; Nanayakkara, A.; Challacombe, M.; Gill, P. M. W.; Johnson, B.; Chen, W.; Wong, M. W.; Gonzalez, C.; Pople, J. A. Gaussian-03 suite of programs; Gaussian, Inc.: Pittsburgh, PA, 2003.
34. ''Spartan '10'' Package, Windows Version, 2011, Wavefunction Inc., USA.
35. P. R. Lowe, C. E. Sansom, C. H. Schwalbe, M. F. G. Stevens, A. S. Clark. J. Med. Chem., 1992, **35**, 3377.
36. K. G. Doucet, J. F. Glister, C. C. Pye. Can. J. Chem. 2010, **8**, 709.
37. P. A. Krieter, , A. E. Colletti, G. A. Doss, , R. R. Miller. Drug Metab. Dispos. 1994, **22**, 625.
38. (a) H. Toufar, K. Nulens, G. O. A. Janssens, W. J. Mortier, , R. A. Schoonheydt, F. De Proft, P. Geerlings. J. Phys. Chem. B. 1996, **100**, 15383. (b) F. De Proft, P. Geerlings. Chem. Rev. 2001, **101**, 1451. (c) P. Geerlings, F. De Proft, W. Langenaeker. Chem. Rev. 2003, **103**, 1793. (d) T. Fievez, N. Sablon, F. DeProft, P. W. Ayers, P. J. Geerlings. Chem. Theory Comput. 2008, **4**, 1065. (e)

G. Roos, P. Geerlings. J. Messens. J. Phys. Chem. B. 2009, **113**, 13465. (f) J. T. Muya, F. De Proft, P. Geerlings, M. T. Nguyen, A. Ceulemans. J. Phys. Chem. A. 2011, **115**, 9069.
39. (a) N. T. Brown, N. Mora-Diez. Phys. Chem. B 2006, **110**, 9270. (b) L. A. M. M. Barbosa, R. A. van Santen. J. Mol. Struct. THEOCHEM. 2000, **497**, 173.
40. P. K. Chattaraj, U. Sarkar, D. R. Roy. Chem. Rev. 2006, **106**, 2065.
41. P. K. Chattaraj, A. Chakraborty, S. Giri. J. Phys. Chem. A. 2009, **113**, 10068.

Table of content:
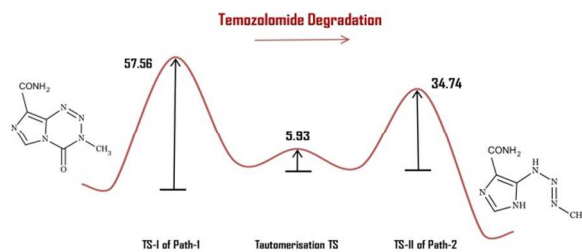
Two pathways for degradation of anticancer agent, Temozolomide were investigateded in which the most energy-favoured mechanism is the combination of the two pathways.